Miloš R. Vasić[1], Filip Pantelić[2], Miloš Vorkapić[3], Anja Terzić[1], Saša Đelević[2], Biljana Ilić[1]*

APPLICATION OF ACOUSTIC EMISSION IN THE BRICK AND TILE INDUSTRY

PRIMENA AKUSTIČKE EMISIJE U CIGLARSTVU

Originalni naučni rad / Original scientific paper
Rad primljen / Paper received: 13.06.2025
https://doi.org/10.69644/ivk-2025-02-0181

Adresa autora / Author's address:
[1)] Institute IMS, Belgrade Serbia
M.R. Vasić https://orcid.org/0000-0002-5743-6038 ;
A. Terzić https://orcid.org/0000-0002-4762-7404 ;
B. Ilić https://orcid.org/0000-0003-0798-1748 ,
[*]email: milos.vasic@institutims.rs
[2)] Academy of Technical and Art Applied Studies, Belgrade, Serbia
F. Pantelić https://orcid.org/0000-0003-4653-9901 ;
S. Đelević https://orcid.org/0009-0007-8318-5117
[3)] University of Belgrade, Institute of Chemistry, Technology and Metallurgy, National Institute of the Republic of Serbia, Belgrade, Serbia M. Vorkapić https://orcid.org/0000-0002-3463-8665

Keywords
- acoustic emission
- drying
- clay
- brick and tile industry

Abstract

The first part of this research focuses on characterising the raw material to assess its suitability for production. The second part explores the use of acoustic emission (AE) as a method for monitoring crack formation during the drying process. Numerous experiments are conducted on heavy clay tile samples to identify acoustic emissions related to physical changes in the material during drying. The impulsive nature of the expected acoustic events suggests broadband excitation, while the wet clay itself strongly attenuates higher frequencies. As a result, the main energy is expected to be concentrated in the lower part of the spectrum. The hypothesis that acoustic events associated with the formation of macro- and micro-cracks fall within the audio frequency range is confirmed. As the brick and tile industry is energy-intensive, this approach supports UN Goal 12 by promoting responsible production and reducing drying scrap rate.

Ključne reči
- akustična emisija
- sušenje
- glina
- opekarska industrija

Izvod

Prvi deo istraživanja je usmeren na karakterizaciji sirovine u cilju provere njene podobnosti za proizvodnju. U drugom delu istraživanja razmatra se upotreba akustičke emisije (AE) kao metode za praćenje pojave pukotina tokom sušenja. Tokom istraživanja obavljeni su brojni eksperimenti na vlažnim uzorcima crepa s ciljem identifikacije akustičke emisije koja prati fizičke promene u materijalu tokom procesa sušenja. Impulsna priroda očekivanih akustičkih događaja sugeriše širokopojasnu pobudu, dok sama vlažna glina kao materijal karakteriše snažno prigušenje viših frekvencija usled čega se očekuje dominantna energija u nižem delu spektra. Postavljena hipoteza da će akustički događaji koji nastaju usled makro i mikroprslina biti locirani u audio opsegu je potvrđena. S obzirom na visoku energetsku zahtevnost industrije opeke i crepa, ovaj pristup doprinosi smanjenju škarta i podržava UN Cilj 12 - odgovornu potrošnju i proizvodnju.

INTRODUCTION

The brick and tile industry is an energy demanding one. Levi and Raut have conducted a life cycle assessment to understand the environmental impact of the brick industry in the West Godavari region of India. It was found that embodied energy varied from 4.9 to 7.8 GJ/m^3, depending on the technology level status /1/. The drying and firing processes are identified as the most intensive in this industry. According to Felea et al., approximately 88 % of the total energy consumption is thermal energy used in the drying and firing processes, /2/. Monroy et al. estimated that the consumption of thermal energy in brick manufacturing in the metropolitan area of Cúcuta, Colombia, is 998 MWh per month. It is also stated that 35 % of all thermal energy is used in the drying process, while the rest of the energy is used in the firing process /3/. Capillary suction, diffusion, and evaporative condensation mechanisms are primarily responsible for transporting liquid water and vapour from the interior to the surface of green products during drying. Besides, in the brick and tile industry, products shrink as drying progresses, and the raw material does not consist of 'pure' clay. Quartz, feldspar, hematite, carbonate (calcite and/or dolomite), and clay minerals (kaolin, illite, montmorillonite, and chlorite) are typically present in the raw material. Listed clay minerals exhibit different drying behaviour. The standard drying sensitivity techniques for comparison of various raw materials are Bigoth, Ratzenberger, Piltz, and Vasić /4-7/. For example, kaolin clays are less sensitive, while montmorillonite ones are swelling and problematic. It is already clear that drying modelling of heavy clay products is not a simple task. Simultaneous heat and mass transfer equations can be solved for different boundary conditions at three modelling degrees (non-conjugated, semi-conjugated, and conjugated) based on the fact that the heat and moisture transport coefficients are determined. The most advanced review about the coupling level for novice and advanced users is recently reported by Perré. 40 years of modelling are expressed in the simple guideline for choosing the best compromise between modelling effort and simulation capabilities. Modelling can be conducted in one, two, or three dimensions (1D, 2D, or 3D) and can involve one, two, or three variables (such as moisture content, temperature, and pressure). If only moisture content is used, these

models have a low physics level. Heat and mass coupling do not exist except when the internal mass transfer is governing the process. Due to the chosen assumptions and used boundary conditions, 2D and 3D modelling for such cases is irrelevant and unnecessary. If moisture content and low temperature are variables, coupling is included. 1D simulation is fast. 2D modelling is recommended and can provide good results. 3D modelling is accurate, but it is not practical due to the unreasonable amount of time necessary for processing and computing. Finally, if all the variables are used and temperatures are high, the coupling is fully included. In this case, 2D and 3D modelling is recommended for use with complex product geometry, especially when anisotropic products are dried or when the moisture content is used to calculate the drying stress, /8/. The technological advances in the brick and tile industry are commonly followed by various patents and innovations that target reduced usage of natural resources, energy savings, and climate neutrality. Furthermore, the lack of scientific papers reporting such technology transfer is evident. Researchers from the German Brick and Tile Institute reported an extremely valuable software, 'ZitroGen' which can be used for modelling the kinetics and energetics of conventional drying, shrinking capillary porous green slabs in counterflow. This model is a semi-conjugated one. Modelling outputs are the evaporation rate, time-dependent moisture, temperature, and shrinkage profiles /9, 10/. Velthuis et al. developed specialised software, 'Drysim' that generates the most suitable industrial drying driving kinetic curve for the tested raw material. This is an upgraded Kitcher receding front semi-conjugated model in which heat and mass transfer coefficients, as well as the fast-drying rate, are experimentally determined on industrial heavy green products, /11/.

Vasić et al. have developed 'Deff calculator' software, used for calculating moisture- or time-dependent effective diffusivity curves under isothermal drying. This is a 2D low-conjugated upgraded diffusional model. It is stated that all internal possible mechanisms that can occur during drying are unambiguously determined on those curves. This served as the basis for modelling real semi-industrial and industrial drying regimes. The drying regime is divided into five segments. Each segment duration is determined from the corresponding isothermal Deff - MR curve /12-14/. The benefits of such development have led the brick and tile industry to relatively easily recognise and adopt well-known global UN Sustainable Development Goals and the EU Circular Economy Action Plan /15, 16/ as necessary over the last two decades. For example, over the last 20 years, the drying time in this industry has been reduced from 42 hours to 21 hours. The most advanced technology now allows for the commercial drying of some hollow clay products in 9 hours. It is important to note that only several raw materials can be used for such production. Acoustic emission (AE) represents transient elastic radiation waves that occur when mechanical energy is released out of the material as a result of the fracture or plastic deformation caused by aging, temperature gradient, or applied mechanical force /17/. For around half a century, the wood industry has successfully used AE for monitoring stress development during drying. Nasir et al. have recently reported the most complete critical review of stated application in this industry /18/. In contrast to the wood industry, the brick and tile industry has not yet adopted AE as a monitoring tool. Additionally, there is a lack of such research. Only a group of scientists from Poland led by J. Kowalski has some experience on this topic. They have isothermally dried pure kaolin clay in the form of a cylinder at temperatures 45, 75, 85, 100, and 120 °C. As already stated, such pure raw material will never be used in the brick and tile industry. Additionally, used temperatures are entirely unsuitable for drying applications in this industry /19/. Nevertheless, the Polish research group is known for its theoretical contribution to drying science. Its mechanistic drying model is outstanding. It provides them with the opportunity to analyse the drying-induced stress and estimate the cracking spot within the drying material /20, 21/. Additionally, they compared mechanistic model predictions with AE to control the drying process /22, 23/. The use of inexpensive piezoelectric sensors, combined with sound card-based logging devices, for registering AE during the drying of heavy clay products would be a promising alternative, given the high cost of accelerometers and ultrasound equipment. In such an application, it is essential to understand that AE signals with frequencies higher than 20 kHz will not be registered. The results of Chen et al. and Duta et al. have led to the assumption that most of the AE peaks during heavy clay drying would be in the sound range of 20 Hz - 20 kHz. Chen et al. have an idea to intensify the drying process using vibrations. They studied the displacement of water inside a capillary tube partly filled with water and subjected to sinusoidal vibration using image analysis. The main idea was that this experimental setup would imitate the conditions of moisture transfer that occur within the pores of porous media during drying. They varied the capillary tube's inner diameter, frequency, and amplitude. The displacement of water due to the asymmetric signal is achieved and confirmed at 30 Hz /24/. Dutta et al. have used AE to analyse the motion of the displacement water front during evaporation of water from artificial microfluidic vessels, inspired by the physiology of vascular water transport in plants. They observed that peaks with the highest resonance in axial and radial direction are respectively 17.2 and 12.7 kHz /25/. In /26/ an AE sensor and setup that directly monitors the formation of microcracks in a clay mixture during the drying process is demonstrated. Furthermore, in /27/ is shown how acoustic emissions are recorded and classified under laboratory conditions in clay rocks, along with an analysis of the time series of impacts and their frequencies. Additionally, the research described in /28/ provides an example of frequency spectrum analysis of AE signals in rocks containing clay minerals, thereby offering important insight into the methodology and parameters for AE recording during the drying process of clay materials. In /29/ is highlighted that electromagnetic interference (EMI), temperature-induced noise in cables, and vibrations from the environment are among the primary sources of signal degradation in structural monitoring and material testing systems. Their systematic analysis shows that environments with active mechanical and thermal components, such as fans, heaters, and power supplies, are

particularly problematic which directly corresponds to the experimental conditions of this research. In /30/ it is demonstrated that simple piezo patch sensors when properly mounted and frequency filtered, can effectively detect AE events in concrete beams. The authors experimentally compared the response of such sensors with commercial AE devices. They demonstrated that successful detection of microfractures and other forms of material degradation depends critically on good mechanical coupling with the sample and the selection of an appropriate frequency range for signal analysis. In /31/, the authors applied deep learning algorithms for fusing AE signals from multiple sensors. Their model enables the detection of AE events masked by noise, based not only on signal amplitude but also on the analysis of the time-frequency structure of signals. This method is particularly suitable for operation in complex acoustic environments, such as drying chambers and thermally active rooms. Besides, recently published work /32/ introduces a pattern for reducing the 'sensor effect' during AE data processing based on descriptor normalisation, statistical tests (Kruskal-Wallis), and multivariate principal component analysis, thereby enabling the creation of reliable signature libraries from multiple sensors. Additionally, the research described in /33/ is important for understanding the characteristics, selection, and calibration of AE sensors for experiments with clay materials. Thus, even with affordable piezo equipment, it is possible to achieve measurements with high sensitivity and reproducibility. The results provide a solid foundation for further expanding the study, including building an AE database and applying machine learning for automatic detection of event types (macro and microcracks) in real time. The primary goal of this study is to verify the applicability of AE for detection of macro and micro cracks during drying of masonry clay elements. The secondary goal is directly related to the challenge of detecting micro impulses during clay drying, where signals are often near the detection threshold. The objective is to create a procedure for filtering and data processing aimed at removing the electric and thermal noise while preserving only AE signals.

MATERIALS AND METHODS

The raw material in this study is taken from the novel deposit of Serbian clay masonry producers. The first step is to characterise the obtained clay. The material is subjected to standard silicate chemical analysis, XRD, TGA and granulometric analyses. After that, the raw material is dried at 60 °C and grounded. A laboratory roller mill is used. The clay is then moistened and processed with laboratory differential mill. Tile specimens 120×50×14 mm are formed on a 'Hendle' type 4 laboratory extruder under a vacuum of 0.8 bar. All drying experiments are done on these tiles. XRD is measured on Philips PW 1440 Cu Kα while DTA is conducted on TA instruments SDT Q 600 form 20 - 1000 °C. Standard SRPS UB1.018 is used for granulometry analysis. Linear shrinkage and weight changes of masonry products are monitored during drying. The dryer is equipped to provide precise control and monitoring, including: air temperature regulation (0-125 °C, ±0.2 °C), relative humidity control (20-100 %, ±0.2 %), airflow adjustment (0-3.5 m/s, ±1 %), as well as continuous weight (0-2000 g, ±0.01 g) and linear shrinkage (0-23 mm, ±0.2 mm) measurements. The Bigoth drying sensitivity and Pfefferkorn plasticity index are also measured. Isothermal (45 °C, RH 50 %, 1 m/s) experiments are conducted on clay tiles to identify acoustic emissions accompanying the physical changes in the material during the drying process. Literature /26-27/ indicates that such phenomena are detected using AE sensors, and a similar methodology is applied in this study. The hypothesis is that acoustic events caused by microcracks would be located within the audible frequency range. The impulsive nature of the expected events suggests broadband excitation, while the moist clay, as a material strongly dampens higher frequencies, thus, energy is anticipated predominantly in the lower part of the spectrum. To identify low-intensity acoustic signals that accompany the occurrence of microcracks during the drying of clay samples, it is essential to minimise all forms of noise and external disturbances present in the measurement system. One of the important decisions in designing the measurement system is to use low-cost piezoelectric sensors (PIEZO-PLS2012 buzzers) previously tested and selected based on response and stability criteria. Calibration Exciter Types 4294 from Bruel & Kjaer is used for sensor testing. This device enables precise adjustment of measurement instruments at a standard acceleration of 10 m/s^2, with a frequency of 159.1 Hz. For this excitation, the piezoelectric sensor produces a sinusoidal voltage signal of 2.8 mV (RMS) at excitation frequency. At frequencies where the sensor is most sensitive (~3500 Hz), the output voltage is about 35 dB higher than at 159.1 Hz, providing a maximal sensitivity of 15.8×10^{-3} Vs^2/m. A sensor attached directly to the mechanical shaker exhibits an amplified response at its resonant frequencies. Mounting sensors on a solid, massive surface diminishes these resonances, providing a more uniform response suitable for measurements when sensors are placed on clay pieces during drying. The sensor response functions are recorded for both cases. The frequency response of the sensor mounted on clay is given in Fig. 1.

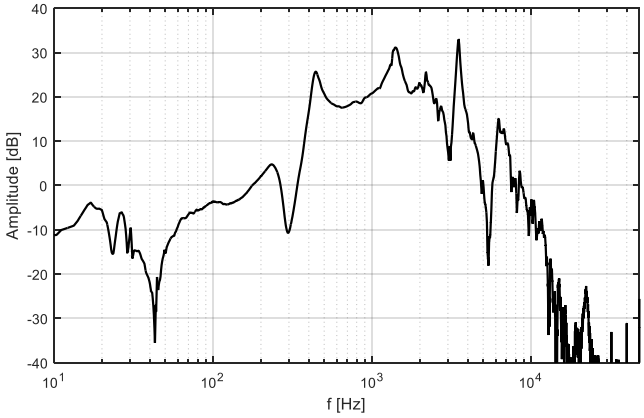

Figure 1. Sensor response to impulsive excitation.

Since the sensor sensitivity is highly nonlinear within the measurement range, the acceleration measured by sensor can be obtained by dividing the measured signal by sensor frequency response function in the complex domain. Returning to the time domain yields the acceleration registered by the sensor. Figure 2 shows the time waveforms before and after

calibration. The signal measured directly at the sensor reaches values of around ±2 mV at specific moments, but over time, its root mean square (RMS) value is much lower. The energy primarily originates from interference induced in the sensor and cables connected to the acquisition system. During testing, it is observed that the polarity of the buzzers varies from piece to piece. Out of 20 sensors tested, those with the most suitable frequency characteristics and highest sensitivity are selected. Pairing of sensors is done with those having the closest characteristics.

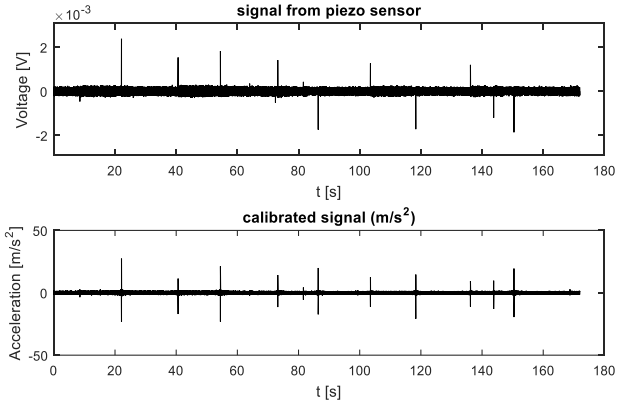

Figure 2. Signal before and after calibration.

RESULTS AND DISCUSSION

Chemical analysis determined the contents of main oxides as follows: 60.41 % SiO_2, Al_2O_3 16.60 %, and 5.99 % Fe_2O_3. Mineralogical analysis identified quartz as the predominant mineral with feldspars present in the form of anorthite. Minerals from the phyllosilicate group are also detected, including micas, kaolinite, illite, chlorite, and smaller amounts of montmorillonite. In addition, minor quantities of carbonates namely calcite and dolomite are identified. Differential thermal analysis (DTA) and thermogravimetric analysis (TGA) further confirmed the presence of small amounts of organic matter and iron hydroxides. Grain size analysis classified the raw material as clayey silt. The clay fraction (< 2 μm) accounts for 30 %, silt (2-60 μm) for 63 %, and sand (> 60 μm) for 7 %. Fine and medium silt (2-20 μm) represents 33 % of the total. Clay composite exhibits high plasticity with a Pfefferkorn plasticity index of 30.82. After processing (grinding, moistening, and homogenisation), the residue on the 10,000 mesh/cm^2 sieve is 7.32 %, and calcium carbonate content is measured at 2.80 %. Drying shrinkage of tested clay tiles ranged from 7.84 % to 8.19 %, indicating a high sensitivity to drying. To monitor the drying process, it is necessary to record even the faintest impulses caused by microcracks. Because these signals can be very quiet, reducing noise in the measurement system is essential. The drying chamber can reach high temperatures which increases thermal noise in connectors and cables. Electromagnetic induction in these components can also be significant due to radiation from the electric motor driving the fan which controls airflow. Computer power supplies have also been observed to affect the noise level in some cases. Initial measurements are conducted with two sensors placed at different positions on the sample. Sensors are glued on the sides which proves to be problematic as they detach due to increased humidity and temperature. Sensors placed on the top surface of the sample prove to be more stable and attaching them with clips is found to be the most effective solution. Additionally, sensors embedded in the sample are tested, yielding promising results but are abandoned because this approach was invasive and caused the sample to crack at locations where sensors were inserted. The example of the AE measuring setup with two sensors is reported in Fig. 3. Two sensors are used for multiple reasons. One is to detect local acoustic events at two distant points, as wave energy could dissipate while travelling through the sample, potentially preventing detection. Another is to determine the position of the acoustic event based on the difference in arrival times of the wave at these sensors, as the wave would reach the closer sensor first. The third reason is to reduce noise by summing or subtracting signals from these sensors, taking into account their different spatial orientations relative to the vertical axis. In the experiment with two sensors on the sample, it is observed that the noise level on the sensor connected to the left channel of the audio interface is 17 dB higher than on the right channel, as shown in Fig. 4. Removing the sensor from the left channel increased the noise on the right channel. This effect means that the 'moist' sample conducts electricity, closing the electrical circuits that influence the noise recorded by the audio interface. It is also noted that the noise level varies during the drying process, likely due to changes in the surface electrical resistance of the sample, resulting from variations in moisture content.

Figure 3. AE measurement setup - two sensors.

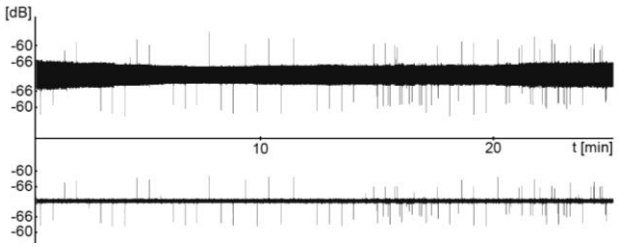

Figure 4. Waveform of left (up) and right (down) channel recordings.

To investigate this, surface electrical resistance is measured during the drying process. Experimental setup is given in Fig. 5, while results are shown in Table 1.

Results show resistance increasing during drying. It is necessary to find a way to reduce the recorded noise. One solution is to connect two sensors in a 'sandwich' configuration with opposite polarities and connect them via balanced audio cables to the interface. This setup is shown in Fig. 6. This configuration significantly reduced system noise.

Figure 5. Surface resistance measurement setup.

Table 1. Resistance measurement.

Time (min)	Moisture content (%)	Surface resistance (kΩ)
0.02	23.52	16.9
4.27	22.84	14.9
5.10	23.02	18.8
10.10	22.87	21.5
15.13	22.60	22.4
20.13	22.22	21.3
25.13	21.79	22.5
30.15	21.51	23.4
35.17	21.07	34.4
40.17	21.41	38.2
45.18	20.12	46.8
50.20	20.64	51.9
55.20	19.52	59.3
60.22	19.18	64.2
65.23	18.61	70.1
70.23	18.18	75
75.25	17.73	79.2
80.27	17.45	83.7
85.27	17.14	86.8
90.28	16.83	90.5

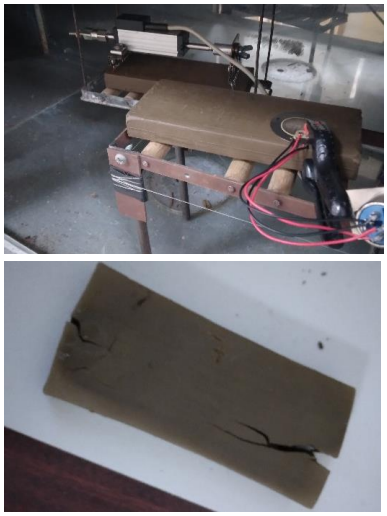

Figure 6. Two sensors connected with a balanced connection.

During measurements, successful detection of acoustic signals corresponding to macrocracks is achieved, as their energy is sufficient to stand out above background noise. The example is shown in Fig. 7.

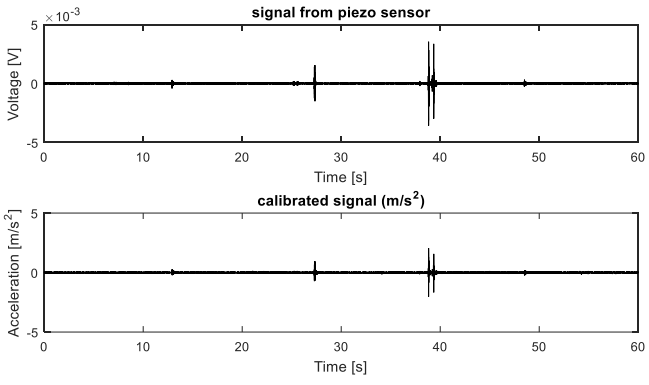

Figure 7. Registered macrocracks.

In addition to these prominent impulses, sequences of weaker impulses are also recorded. This phenomenon motivates a more detailed analysis focused on the detection and quantification of low-intensity acoustic events. A special

algorithm is developed in the digital domain to detect all impulses that exceed a set threshold. After calculating RMS value of the entire signal, the threshold is set 18 dB above it. Moments in time when values exceeded this threshold are detected and labelled with a number. Figure 8 shows the waveform of a signal with marked peaks exceeding the threshold, indicated with red and blue dots. One way to quantify those impulses is to track their energy. Recorded electrical voltages from sensors are squared, and the resulting energy measure is proportional to these values, expressed in μV^2. Cumulative energy is calculated separately for positive and negative peaks (indicated in blue and red). To minimise the influence of noise, only segments that exceed the threshold are summed. The signal is pre-filtered with a low-pass filter at 20 kHz. The result of this procedure is shown in Fig. 9.

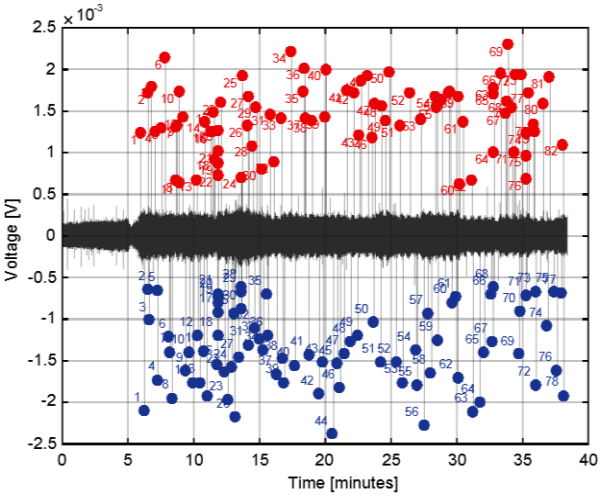

Figure 8. Identification of low-amplitude impulses.

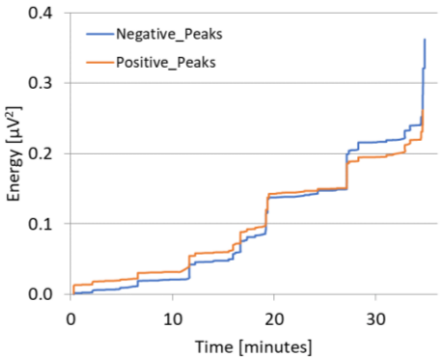

Figure 9. Cumulative energy of low-amplitude impulses.

This diagram is important since it can be used for visualisation of crack appearance during drying, since energy jumps correspond to the occurrence of micro- and macro cracks. If results are compared with Fig. 7 it is clearly seen that macrocrack is formed exactly at the same moment at 28 min. It is important to state that from the moment of macrocrack formation the energy of negative peaks is above the energy of positive peaks. This pattern can be used for precise distinguishing the appearance of microcracks from macrocracks during drying. It is important to note that in some samples, what initially looks as impulses from microstructural changes (micro-splitting or micro-expansion), proves to have a completely different nature. The specific characteristics, their precision, extreme transience, and high-frequency content of such signals indicates electrical- rather than mechanical origin. Besides, the sensors used could not register mechanical events with such high-frequency content.

Further analysis reveals that these impulses result from sudden changes in the electric field. Their frequency of occurrence suggests a possible link to the electrical circuit powering the heater inside the dryer. To test this, signals are recorded simultaneously from a piezoelectric sensor inside the dryer and from a microphone positioned near the electro-mechanical switch board that activates the heater. It is determined that the acoustic signal from the switch board is not of sufficient amplitude to affect measurements via sound transmission through air. However, the sudden jump in the electric current when the heater is turned on induces an impulsive signal in the piezoelectric sensor which, in this case, acts as an antenna. The presence of a 50 Hz mains voltage component with characteristic harmonics was also observed in the signals. The procedure similar to the one described in /32-33/ is used to eliminate these unwanted impulses and to improve the process of identifying weaker signals that occur in parallel with macrocracks. Using a band-pass filter (3-20 kHz), low-frequency interference from the mains power supply is removed, and high-frequency transients of the unwanted signals are suppressed. Results are reported in Figs. 10 and 11.

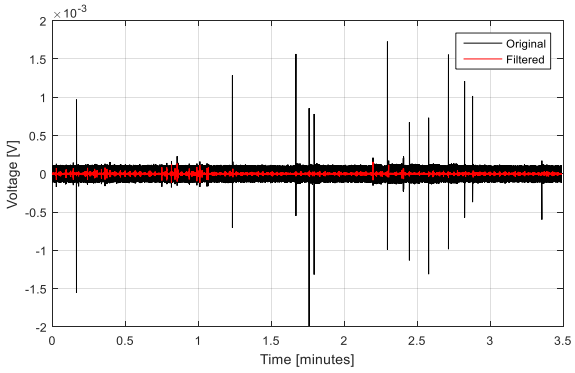

Figure 10. Signal segment before and after applying band-pass filter (3-20 kHz).

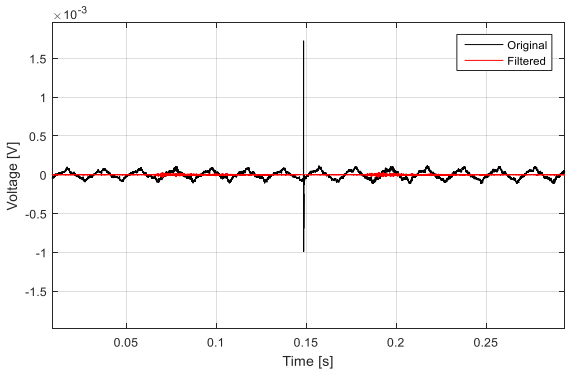

Figure 11. Detail of low-amplitude impulse, before and after filtering (3-20 kHz).

Filtering removed noise associated with the power supply which appears as a characteristic triangle wave in Fig. 11. This filter also suppressed high-frequency components responsible for the transient. After filtering, segments with lower amplitude, longer duration, and different spectral content are revealed. Example of such signal is given in Fig. 12.

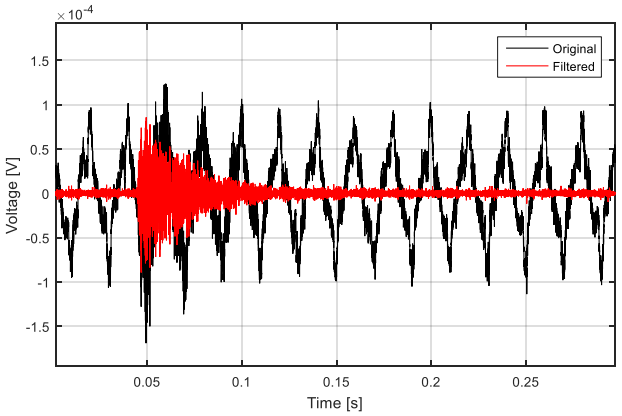

Figure 12. Impulse of non-electrical origin.

Recording such signals is challenging because the events of interest have very low energy within equipment measuring range. Low signal levels, combined with noise, vibrations, and electromagnetic interference, pose significant difficulties. Automatic identification of these impulses requires the development of additional algorithms. Unlike the high-frequency, intense, and short electrical impulses, the signal of our interest has lower amplitude and longer duration. Various methods for classifying signals are tested to detect each occurrence of this type. The median of 3 ms segments is identified as the most effective feature for identification. The procedure involved:

- filtering with a band-pass filter (5-11 kHz),
- calculating the median of the hole signal using the 3 ms window,
- using this median as a parameter for separating sharp electric impulses from longer mechanical ones since the median remains low for the former and increases for the latter,
- creating a logical function (values 0 or 1) that activates when the median exceeds a set threshold (e.g., 2×10^{-6}). It is important to note that the logical function activates only during acoustic emission events. It remains zero when electric impulses are found. Example of signal processing is reported in Fig. 13.

This approach has a strong literature background, e.g., an unsupervised skip neural network methodology for noise reduction in AE signals is developed in /34/, with a specific focus on nonlinear distortions and impulsive noise. Their results indicate that combining basic statistical descriptors (such as the median) with more complex nonlinear filters can significantly improve the detection of weak AE impulses in real-time, even at low signal-to-noise ratios. Additionally, research described in /35/ emphasizes the need to integrate time-frequency analysis and monitor electromechanical changes in the material, being particularly relevant in conditions of variable temperature and humidity.

These factors, identified in our experiment as sources of surface resistance changes in clay, directly affect the acoustic transmissibility and electromagnetic sensitivity of the system. Signal processing proposed in this study shows that it is possible not only to filter and classify AE events but also to understand their causal relationship with physical changes in the material. The combined findings suggest that practical AE analysis can be achieved even with simple equipment, as long as careful signal processing is applied. Future work will be focused on creating a comprehensive database of AE patterns under various drying condition for this clay. This database is planned to be a crossover with the authors effective diffusivity vs. moisture content database and serve as a base for machine learning algorithms for detection of microcracks and the prevention of macrocracks.

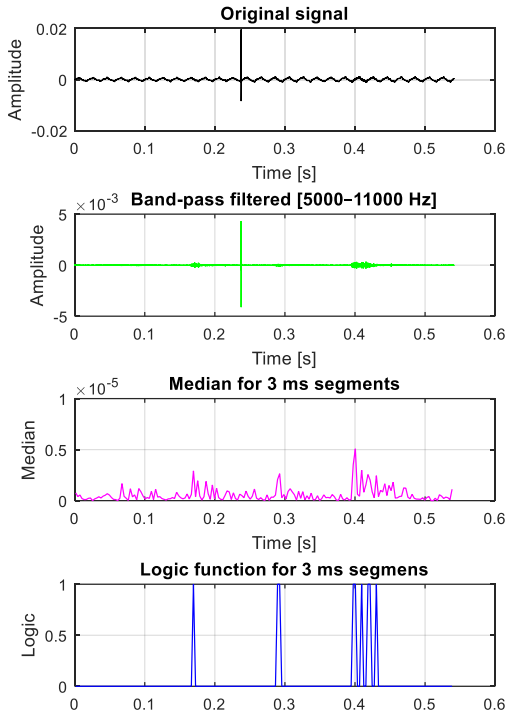

Figure13. Example of data processing output.

CONCLUSION

The study demonstrates that AE monitoring is a viable method for detecting micro- and macrocrack formation during the drying of clay masonry products, even when using low-cost sensors and simple data acquisition systems. The successful identification of acoustic signals related to physical changes in the material confirms that with proper calibration, filtering, and signal processing, critical events can be captured despite high background noise and interference typical in industrial drying environments. The developed methodology enables the differentiation between mechanical AE signals and electrical or thermal noise through advanced signal filtering and statistical classification techniques. Notably, the use of median based signal segmentation proves effective in isolating weak AE events associated with microcrack formation, paving the way for more reliable real-time monitoring. The observed correlation between AE signal energy and crack severity supports the potential for early detection and classification of damage during drying. This research provides a strong foundation for the future development of an AE signal database that can be cross-referenced with effective diffusivity data. This research has the potential to significantly reduce drying-related defects, energy consumption, and material waste in the brick and tile industry, contributing to more sustainable manufacturing practices.

ACKNOWLEDGEMENTS

This work is financially supported by the Ministry of Science, Technological Development and Innovation of the

Republic of Serbia, NITRA (Contracts No.: 451-03-136/2025-03/200012 and 451-03-136/2025-03/200026). Goal of this work aligns with SDGs (especially SDGs 9, 11, 12, and 13).

REFERENCES

1. Levi, K.P., Raut, A. (2021), *Embodied energy analysis to understand environmental impact of brick industry in West Godavari region*, Mater. Today: Proc. 47(15): 5338-5344. doi: 10.1016/j.matpr.2021.06.061
2. Felea, I., Bendea, G., Rancov, N., et al. (2021), *Energy performance level analysis of a brick manufacturing process*, J Sustain. Energy, 12(1): 40-51.
3. Monroy, R., Romero Y.A., Gelves, J.F. (2018), *Consumption of energy in the manufacturing of ceramic bricks in the metropolitan area of Cúcuta, Colombia*, J Phys.: Conf. Ser. 1126: 012014. doi: 10.1088/1742-6596/1126/1/012014
4. Bigot, A. (1921), *Retrait au séchage des kaolins et argiles*, Report of Academy of Sciences, Paris
5. Ratzenberger, H. (1990), *An accelerated method for the determination of drying sensitivity*, Ziegel Ind. Int. 43(6): 348-354.
6. Piltz, G. (1971), *Technical parameters of drying heavy clay raw materials*, Ziegel Ind. Int. 24(7): 294-300.
7. Vasić, R.M. (2022), *Estimation of the drying behavior for different clay raw materials - drying sensitivity techniques review*, J Silic. Based & Compos. Mater. 74(3): 88-92. doi: 10.14382/epitoanyag-jsbcm.2022.14
8. Perré, P., Rémond, R., Almeida, G., et al. (2023), *State-of-the-art in the mechanistic modeling of the drying of solids: A review of 40 years of progress and perspectives*, Drying Technol. 41 (6): 817-842. doi: 10.1080/07373937.2022.2159974
9. Telljohann, U., Junge, K., Specht, E. (2008), *Moisture diffusion coefficients for modeling the first and second drying sections of green bricks*, Drying Technol. 26(7): 855-863. doi: 10.1080/07373930802136053
10. Junge, K., Tretau, A. (2007), *Increasing the energy efficiency of drying plants through the use of modern low-energy dryers*, Ziegel Ind. Int. 60(9): 22-31.
11. Vellhuis, J.F.M., Denissen, J. (1997), *Simulation model for industrial dryers: reduction of drying times of ceramics & saving energy*, Drying Technol. 15(6-8): 1941-1949. doi: 10.1080/07373939708917339
12. Vasić, M., Grbavčić, Ž., Radojević, Z. (2014), *Analysis of moisture transfer during the drying of clay tiles with particular reference to an estimation of the time-dependent effective diffusivity*, Drying Technol. 32(7): 829-840. doi: 10.1080/07373937.2013.870194
13. Vasić, M., Rekecki, R., Radojević, Z. (2018), *Procedure for setting up the drying regime that is consistent with the nature and properties of the clay raw material*, Drying Technol. 36(3): 267-282. doi: 10.1080/07373937.2017.1324879
14. Vasić, M., Radojević, Z. (2018), *Update of the procedure used for heavy clay dryer optimization*, Rom. J Mater. 48(4): 436-441.
15. https://sdgs.un.org/goals (last accessed 21.08.2025)
16. https://eur-lex.europa.eu/legal-content/EN/TXT/?qid=1583933814386&uri=COM:2020:98:FIN (last accessed 21.08.2025)
17. Spanner, J.C., McElroy, J.W. (Eds.), Monitoring Structural Integrity by Acoustic Emission, STP571-EB, ASTM International, 1975. doi: 10.1520/STP571-EB
18. Nasir, V., Ayanleye, S., Kazemirad, S., et al. (2022), *Acoustic emission monitoring of wood materials and timber structures: A critical review*, Constr. Build. Mater. 350: 128877. doi: 10.1016/j.conbuildmat.2022.128877
19. Vasić, M., Radojević, Z. (2020), *Characterization of drying behavior and modeling of industrial drying process*, IOP Conf. Ser.: Mater. Sci. Eng. 916: 012124. doi: 10.1088/1757-899X/916/1/012124
20. Kowalski, S.J., Thermomechanics of Drying Processes, 1st Ed., Springer Berlin, Heidelberg, 2003. doi: 10.1007/978-3-540-36405-4
21. Kowalski, S.J., Rybicki, A. (2006), *The vapour-liquid interface and stresses in dried bodies*, In: Kowalski, S.J., Rybicki, A. (Eds.) Drying of Porous Materials, Springer Dordrecht. doi: 10.1007/978-1-4020-5480-8_5
22. Kowalski, S.J., Pawłowski, A. (2010), *Drying of wet materials in intermittent conditions*, Drying Technol. 28(5): 636-643. doi: 10.1080/07373931003788718
23. Kowalski, S.J. (2010), *Control of mechanical processes in drying. Theory and experiment*, Chem. Eng. Sci. 65(2): 890-899. doi: 10.1016/j.ces.2009.09.039
24. Chen, W., Colin, J., Casalinho, J., et al. (2018), *Drying intensification by vibration: fundamental study of liquid water inside a pore*, In: 21st Int. Drying Symp. IDS'2018, Valencia, Spain, Editorial Universitat Politèknika de Valencia, pp.1911-1918. doi: 10.4995/ids2018.2018.7961
25. Dutta, S., Bieling, T.J., Verbiest, G.J. (2023), *Evaporation induced acoustic emissions in microfluidic vessels*, R. Soc. Open Sci. 10(12): 231029. doi: 10.1098/rsos.231029
26. Kouta, N., Saliba, J., Saiyouri, N. (2021), *Monitoring of earth concrete damage evolution during drying*, Constr. Build. Mater. 313: 125340. doi: 10.1016/j.conbuildmat.2021.125340
27. Fieseler, C., Mitchell, C.A., Pyrak-Nolte, L.J., Kutz, J.N. (2022), *Characterization of acoustic emissions from analogue rocks using sparse regression-DMDc*, J Geophys. Res.: Solid Earth, 127(7): e2022JB024144. doi: 10.1029/2022JB024144
28. Yan, J., Li, Z., Xia, D., et al. (2024), *Influence of immersion time on the frequency domain characteristics of acoustic emission signals in clayey mineral rocks*, Materials, 17(13): 3147. doi: 10.3390/ma17133147
29. Hassani, S., Dackermann, U. (2023), *A systematic review of advanced sensor technologies for non-destructive testing and structural health monitoring*, Sensors, 23(4): 2204. doi: 10.3390/s23042204
30. Cazzulani, G., Alexakis, H. (2024), *Comparison between acoustic emission sensors and piezoelectric patches for damage detection in concrete beams*, In: Proc. 10th Eur. Workshop on Structural Health Monitoring (EWSHM 2024), Potsdam, Germany, e-J Nondestr. Testing, 29(7). doi: 10.58286/29827
31. Cheng, L., Nokhbatolfoghahai, A., Groves, R.M., et al. (2024), *Data level fusion of acoustic emission sensors using deep learning*, J Intell. Mater. Syst. Struct. 36(2): 77-96. doi: 10.1177/1045389X241291439
32. Chen, X., Godin, N., Doitrand, A., Fusco, C. (2024), *Reduction in the sensor effect on acoustic emission data to create a generalizable library by data merging*, Sensors, 24(8): 2421. doi: 10.3390/s24082421
33. Wu, R., Selvadurai, P.A., Chen, C., Moradian, O. (2021), *Revisiting piezoelectric sensor calibration methods using elastodynamic body waves*, J Nondestruct. Eval. 40(3): 68. doi: 10.1007/s10921-021-00799-1
34. Wulan, T., Li, G., Huo, Y., et al. (2024), *Study of acoustic emission signal noise attenuation based on unsupervised skip neural network*, Sensors, 24(18): 6145. doi: 10.3390/s24186145
35. Tai, J.L., Sultan, M.T.H., Łukaszewicz, A., et al. (2025), *Preventing catastrophic failures: A review of applying acoustic emission testing in multi-bolted flanges*, Metals, 15(4): 438. doi: 10.3390/met15040438